PREAMBLE

1. The urgency of the thesis topic

In the world, scientists have to do experiments to determine the design parameters for the flow distribution grille and have to do experiments to determine the specifications when installing the air flow distribution grille to put into operation. In Vietnam, it has made it difficult for the plants to take the initiative to replace the repair. Especially when changing fuel, changing the air discharge and changing precipitation system. ***The research in order to identify the specifications of the air flow distribution grille in the electrostatic precipitators to improve precipitation efficiency*** " is a matter of high scientific and practical significance in Vietnam today.

2. Objectives of the research:

- Theoretical research on the effect of air speed level on the dust filtration efficiency combined with empirical research on the model to determine the influence of some specifications of the flow distribution grille to the air speed level;
- Verification of the experimental results on industrial electric precipitators.

3. Research subjects:

The object of the research is to experiment on the electrostatic precipitators model to determine the effect of some specifications of the flow distribution grille to the airflow speed level and then to test the efficiency of the industrial precipitators with the capacity of 55 MW based on the application of 01 plan with good level achieved on the experimental model.

4. Research scope:

- An overview of dry electric dust precipitation technology;
- Nghiên cứu cơ sở lý thuyết về ảnh hưởng mức đều của vận tốc khí tới hiệu suất lọc bụi của the dry electrostatic precipitator;
- Experiment to find the solution to create the level of speed field on the model by mechanical method is to adjust some specifications of airflow grille such as position of grille installation, the number of grille installated at the same time, grille in two forms of square and round holes. In which, for the ventilation coefficient, choose f = 45% [14, 15], then verify 01 plan with the good level on the dry industrial electrostatic precipitators with a capacity of 55 MW.

5. Research methodology

- Theoretical research combined with experimental research on the model to determine the influence of some specifications of the flow distribution grille to the levle of the airflow speed while verifying the experimental results of the model into the industrial electrostatic precipitator;
- Use of the least squares method to evaluate the experimental results.

6. The scientific and practical significance of the thesis results

6.1. Scientific significance:

- Determining that the mechanical solution is to adjust some main specifications of the flow distribution grille, to create a level of speed of 10% -15%;
- The experimental results have diversified the airflow distribution grille with the square hole system that can be applied to the grille design for electrostatic dust precipitation, not only depending on the type of grille with round hole system;
- The research results above can be used as a basis for the research and application of electrostatic precipitators with different capacity.

6.2. Practical significance

- The result has been verified to install a symmetrical grille with the ventilation of 45%, round hole system on the device is industrial electrostatic precipitators with a capacity of 55MW for dust precipitation efficiency of 99.2%;

- Results can be used as a basis for research and applied to electrostatic precipitators of different capacities;

The cost of making grille and materials with high mechanical properties, the same section of square hole system is only 40% of the production cost of the round hole system.

7. New contributions

The first in Vietnam, by theoretical research combined experiment, it has found a mechanical solution to create the level of air speed on the model of the chamber of electrostatic precipitators on the basis of adjusting some specifications of the square and round hole distribution grille system with the ventilation of 45%, has proven to improve dust precipitation efficiency when installing 01 symmetric grille at the inlet and outlet on the electrostatic precipitators of industrial coal dust with a capacity of 55MW.

Chapter 1: OVERVIEW OF ELECTRIC DUST PRECIPITATION TECHNOLOGY

1.1. Schematic structure and working principle of electric precipitators

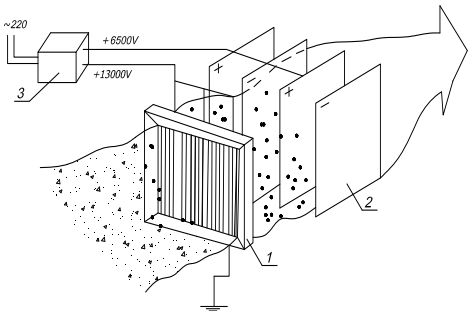

Figure 1.3. Diagram of principle of precipitator

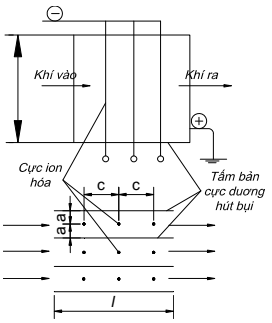

Figure 1.2. Two-zone electric precipitator

1.2. Classification of dry electrostatic precipitators

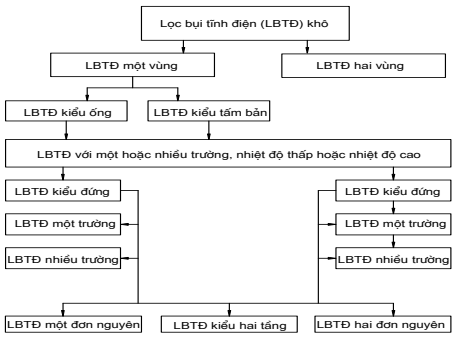

Figure 1.5. Classification of dry electrostatic precipitators

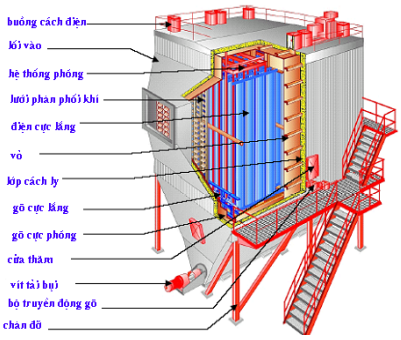

Figure 1.8. Structural diagram of the horizontal electrostatic precipitator

1.3. The concept of dry electric dust precipitation

Dust precipitation in which air cleaning occurs at the temperature higher than the dew point, so that the dust is always in dry state.

1.4. Structural principles of electrostatic precipitators

Shown in Figure 1.8

1.5. Efficiency of electrostatic precipitators

1.5.1. Equation of electrostatic precipitators

v_{max} - maximum speed of airflow:

$$v_x = \frac{dx}{d\tau} = v_{max}(1 - \frac{y^2}{R^2}) \qquad (1.1)$$

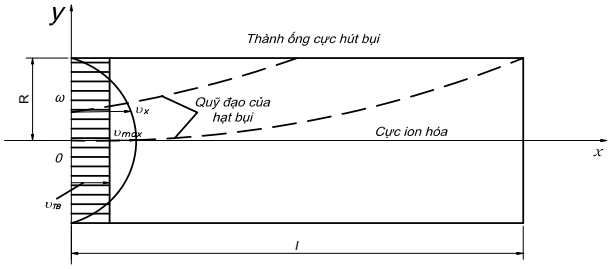

Figure 1.9. Diagram of pipe-type electric precipitator

1.5.2. Precipitation efficiency by particle size of electric precipitators

$$\eta = \frac{C_1 - C_2}{C_1}$$

Precipitation efficiency - the first and final concentration of air dust through the precipitator

Plate type: $\eta = 1 - \exp(-\frac{\psi\omega l}{av})$

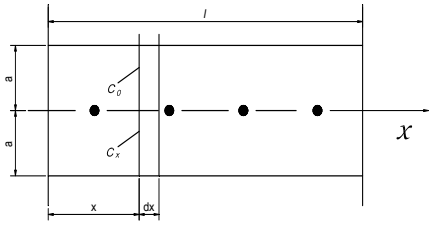

Figure 1.10. Flow chart of precipitation efficiency calculation

1.6. Factors affecting the efficiency of electrostatic precipitators

a) The characteristic of the air needs to be cleaned

b) Effect of dust layer resistivity

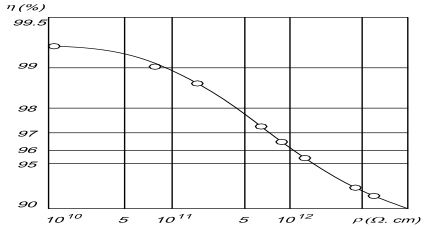

Figure 1.13. Influence of resistivity

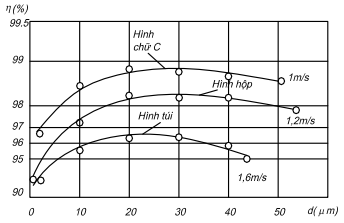

Figure 1.12. Influence of dust particle size

đ) Effect of temperature on precipitation efficiency

e) Effect of moisture on efficiency

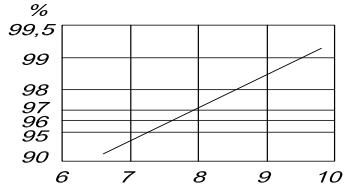

Figure 1.15. Correlation between efficiency and moisture

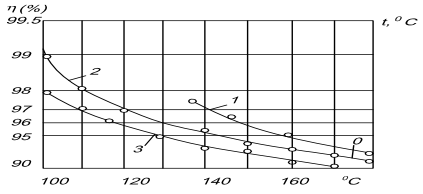

Figure 1.14. Influence of temperature

h) Influence of speed of dust element movement on precipitation efficiency

$$\eta = e^{-vA/Q} \qquad (1.24)$$

Comment: The precipitation efficiency (η) of the electric device depends on the main parameters such as speed (ω) and diameter (δ) of dust particles, speed (v) of airflow, the flow of airflow (L), the length of the precipitation chamber (A), the section of the precipitation plate,... However, no research has investigated the effect of air speed level (v) on precipitation efficiency (η).

1.7. Domestic research on electric precipitators

1.8. Research in the world on the effect of airflow speed field on precipitation efficiency of electric precipitators

- Author I. C. Riman [12]: has investigated the effect of air resistance balance

- G.A.Gygienco [14]: Adjust the speed level of the airflow

- Elder [26]: by experiment, found a linear constraint between the speed levle and the characteristics of the flow distribution grille;

- Scientist Mak-Charter [27]: has established the equation of the resistance of flat air distribution grille;

- Some experimental studies 1946-1948 [7]: opening angle α1=24-180^o;

- Research Institute of Industrial Emissions of Russia (Niiogaz) 1954: Researched on the experimental model to create an even airflow distribution [23], [24], [25];

- Doctor of Science I.E. Ideltric (1983): verified on the model, the precipitation efficiency dependence on the the air speed level by experiment [13], [15].

Conclusion of Chapter 1:

1. A review of the research on the technology and equipment of dry precipitation, which are widely used in coal-fired power plants in Vietnam.;
2. The main factors affecting the precipitation efficiency of the device including: airflow speed, input dust content, level of speed in the precipitation chamber, air humidity, resistivity, air precipitation properties, temperature, ...;
3. Recent research by scientists in the world suggests that the level of air speed can be created *by the mechanical method of adjusting some of the specifications of the airflow distribution grille*;
4. The topic has selected the method of combining theoretical and experimental research to determine the influence of some specifications of the airflow distribution grille to the level of the speed in the precipitation chamber to improve dust precipitation efficiency.

CHAPTER 2: THEORETICAL BASIS FOR THE FACTORS AFFECTING THE EFFICIENCY OF ELECTRIC DUST PRECIPITATION

2.1. The general mechanical concept of dust

2.1.1. Dust and classification

Coarse dust, sand dust (grit): particle $\delta > 75\mu m$**;** Dust (dust): solid particles $(5 \div 75\mu m)$**;** Smoke: particle size $\delta = 1 \div 5\mu m$**;**- Fume (fume): particles $\delta < 1\mu m$**;** Mist (mist): liquid particle size $\delta < 10\mu m$.

2.1.2. Resistance of solvent motion of particles

a) Particles moving with constant speed

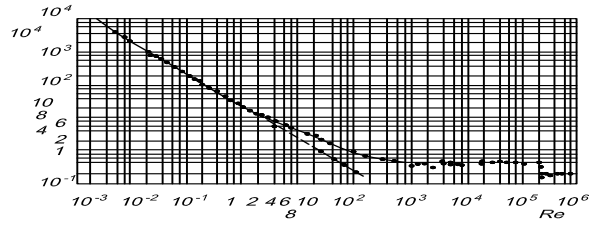

Figure 2.1. The resistance factor does not depend on the Raynon coefficient (Re), [33]

Spherical particles with a diameter of δ moving in the solvent with speed of v the resistance F of the solvent affecting on the particle [39]: $F = K_0 A \frac{1}{2} \rho \upsilon^2$ (2.2)

In which: $\frac{1}{2}\rho\upsilon^2$ - kinetic energy; A – area of the direct cross section of the particle;

K_0 - coefficient of dependence on the Re coefficient (figure 2.1) [3]; ρ - unit mass per substance.

Sisk F.J. [20] has drawn the experimental formula with the error $\approx 2\%$ in a very wide range of Re value (0,1 < *Re* < 3500):

$K_0 = 29{,}6\,\mathrm{Re}^{(0{,}554 In\,\mathrm{Re} - 0{,}983)}$ (2.9)

In the general case, the direct resistance of the solvent affecting the particle when moving has the acceleration represented by the following equation (2.25):

$$F_a = P - ma = 3\pi\mu\delta\upsilon + \frac{\pi}{12}\rho\delta^3 a + \frac{3\delta^3}{4}\sqrt{\pi\mu\rho}\int_0^{\tau}\frac{d\upsilon}{dx}\frac{dx}{\sqrt{\tau - x}}, \qquad (2.25)$$

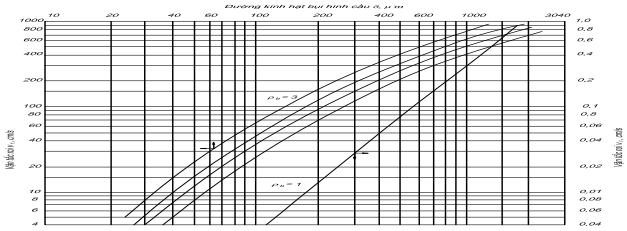

Figure 2.3. Fall speed of particles

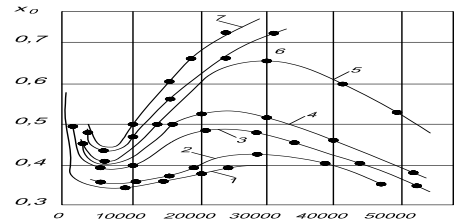

Figure 2.4. resistance coefficient when moving

2.1.3. Aerodynamic resistance when multiple particles move together

According to Hawksley [40], the movement resistance of many dust particles is determined by the formula:

$$F_o = F(1-C)^{-4,65} = aF \qquad (2.30)$$

or: $$F_o = F(1+4{,}65C) = bF \qquad (2.31)$$

2.1.4. Settle of dust particles from tangled motion

From the congruent method, we get (2.34):

$$f\left(\frac{N_o}{u_\tau C}, \frac{u_\tau \delta}{\nu}, \frac{\rho_b}{\rho}, \frac{D_{Br}}{\nu}\right) = 0 \qquad (2.34)$$

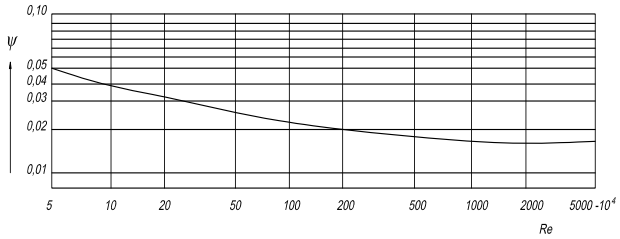

Figure 2.5. Friction coefficient ψ depending on R_e

2.1.5. Influence of particle shape

Comment: Fundamentals of mechanical theory of dust can be commented as follows:

- The speed of the dust depends on the flow regime of the solvent, typically the Reynon coefficient (Re);

- The speed of the particle depends on the characteristics of the particle itself, such as: moving environment, particle shape, particle roughness, particle mass and depending on the environment with many particles in motion...

- In fact, the speed depends on the structure of the air channel, obstructions in the air channel due to the structure of the device.

2.2. Characteristics of the airflow in the channel

Ideal kinetic energy ratio and airflow momentum K_{lt}/K_k according to the average speed ω_k is the Bysinesk coefficient, called the level of the speed field under the formula (2.4), [26]:

$$M_k = \frac{K_{lt}}{K_k} = \frac{\rho\int_{F_k}\omega^2 dF}{m\omega_k} = \frac{\int_{F_k}\omega^2 dF}{\omega_k{}^2 F_k} = \frac{1}{F_k}\int_{F_k}\bar{\omega}^2 dF \qquad (2.49)$$

This shows the level coefficient of speed $M_k \geq 1$ and $N_k \geq 1$ [10,11, 23] these coefficients are greater than 1, the higher the level of speed on the cross section.

So always $N_k > 1$ when $|\Delta_\omega| \neq 0$. Similarly, the momentum coefficient M_k is:

$$M_k = 1 + \frac{1}{F_k}\int_{F_K}\Delta\bar{\omega}^2 dF = 1 + \delta'_\omega \qquad (2.52)$$

Which means that: $M_k > 1$ when $|\Delta_\omega| \neq 0$.

Combining formula (2.52), establish relationship M_k and N_k we get:

$$N_k \approx 3M_k - 2. \quad (2.53)$$

In case $N_k >< 3M_k$-2 [12] the more accurate formula of N_k is:

$$N_k = 3M_k - 2 + \frac{1}{F_k}\int_{F_k} \Delta\bar{\omega}^3 dF. \quad (2.54)$$

2.3. Characteristics of the structure of the airflow speed in the straight channel

a) Concept: The airflow speed in the channel at the channel section of the large scale curve of the speed represented by the straight line with the arrow (fig. 2.6), [46].

b) Characteristics

People experimented with different ratios (x) and air pipe diameter Dk, the speed chart also changes as shown in the figure 2.6:

In the flow mode of graphical plane of airflow speed c in the parabolic form (figure 2.6a), the formula is (2.54):

$$\frac{\omega}{\omega_{\max}} = 1 - (\frac{y}{R_k})^2 = 1 - \bar{y}^2 \quad (2.54)$$

The dependence of speed on the inlet structure

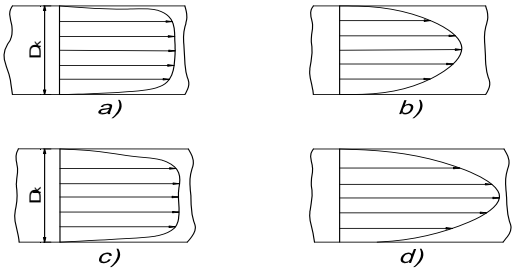

Figure 2.6. The speed on cross section of straight pipe a) x/D_k=13,6; b) x/D_k =24,2; c) x/D_k = 38,4; d) x/D_k=51,8,

c) The dependence of speed on the channel structure

2.4. The method of assessing the influence of the speed field level on the filter efficiency of the device

2.4.1. Some main formulas

- Average dust emission factor $\bar{g}_{yh}$, [47]: $\bar{g}_{yh} = \frac{g_{yh}}{g_{nx}} e^{(-k_1\omega)^{-1}}$ (2.56)

- Filter efficiency η: $\eta = 1 - \bar{g}_{yh} = 1 - e^{(-k_1\omega)^{-1}}$ (2.57)

From that calculating k_1: $k_1 = \left(-\omega l_n \bar{g}_{yh}\right)^{-1}$ (2.58)

Apply for electrostatic precipitator, calculating k_1 according to Deich, [16]: $k_1 = \frac{\delta}{(cE_1 l_э)}$ (2.59)

Pollutant dust content and average efficiency:

- The average value of the dust emission factors as uneven distribution speed (ω) [7]:

$$\left(\bar{g}_{yh}\right)_\omega = \frac{1}{F_k}\int_{F_k} \bar{g}_{yh}\bar{\omega} dF. \quad (2.60)$$

Efficiency: $$\eta_\omega = 1 - \left(\bar{g}_{yh}\right)_\omega = 1 - \frac{1}{F_k}\int_{F_k} \bar{\omega} e^{\left(-k_1\omega_k\bar{\omega}\right)^{-1}} dF. \quad (2.61)$$

- When evenly distributed speed we have $\omega = \omega_k$ then dust emission factor is determined, [7]: $$\left(\bar{g}_{yh}\right)_k = e^{(-k_1\omega_k)^{-1}} \quad (2.62)$$

Calculate the even distribution coefficient M_k, on a round section and flat section:

- Round section: $M_k = 2\int_0^1 \bar{\omega}^2 \bar{y} d\bar{y} = \int_{-1}^1 \bar{\omega}^2 \bar{y} dy$ (2.63)

- Rectangular section: $M_k = \int_0^1 \bar{\omega}^2 d\bar{y} = 0,5\int_{-1}^1 \bar{\omega}^2 d\bar{y}$ (2.64)

Uneven distribution coefficient M_k [17]: $\omega'_k = \frac{\int_{F_k} \omega^2 dF}{\int_{F_k} \omega dF} = \frac{\int_{F_k} \omega^2 dF}{\omega_k F_k} = \frac{\omega_k}{F_k}\int_{F_k} \bar{\omega}^2 dF = M_k \omega_k$ (2.65)

From (3.10) we have: $M_k = \frac{\omega'_k}{\omega_k} = \frac{\omega'_k F_k}{(\omega_k F_k)} = \frac{Q'}{Q}$

In which: ω'_k the average speed is calculated by the ratio between the amount of dust emission Q' and the total air consumption Q flowing through the same section

Comment: On the effect of the speed field level in cross-section of the filter chamber on the equipment efficiency: According to [7], the influence of speed field level is very large, even when $M_k = 1,31$ then dust emission has increased 2 times.

2.4.2. Balancing mechanism of airflow resistance

a) Airflow distribution unit

- *Small level:* the adjustment mechanism has very small opening angle, suitable for channel of straight pipe;
- *Large level:* is the level of air inlet with large opening angle (α_1= 8 - 90^o), in case of long channel then α_1<8^o;
- *Full level:* Inlet with a opening angle increased suddenly, α_1>90^o, the characteristic of the airflow is that there is no translational particle on the majority of the cross section.

b) Classification of airflow resistance

- *Critical resistance* is the resistance required to achieve a level of the speed field;
- *Consumption resistance* is the actual resistance that arises when the airflow flows through the flow divider.

c) Resistance balance method

- Determination of the critical resistance coefficient of the air distribution grille: $\xi_{kr} = \frac{2\delta p_p}{\rho \omega_p^2} = \xi_{opt}$;
- Determination of optimal resistance coefficient (ζ_{ont}) of the flow distribution unit means that the resistance coefficient makes airflow evenly distributed over the whole channel section.

2.5. Some solutions to improve the efficiency of electric precipitators

- *Select the optimum air speed:* select according to experience, more accurate method is to use experimental methods, [56];
- *Select the opening angle of the air supply channel:* Opening angle of the inlet [58], it is capable of directing airflow into the center of the filter chamber, increasing the filter efficiency of the device;
- *Adjust the flow divider*:
- *Adjust the airflow direction:* Direct the dust airflow into the center of the filter chamber: according to [13] the center of the filter chamber is capable of collecting up to 90% of the dust through the filter chamber.
- *Suitable grille type:* For example, flat grille, round holes, rectangular holes, granular materials, etc., all directly affect the level of speed and the make improvement of the dust filter efficiency of the device, [52].

Conclusion of chapter 2

1. Resistance to dust in the moving solvent includes the following factors: Re coefficient, particle characteristics such as shape, surface roughness, mass, amount of dust involved in moving in the solvent...;
2. The level of the air speed in the filter chamber (deviation between small velocities) on the basis of a reasonable change in the specifications of the airflow distribution grille such as type, quantity, relative installation location between airflow distribution grilles, resulting in improvement of filter efficiency of the electric device;
3. The level of the air speed in the filter chamber is improved on the basis of changing the technical parameters of the air inlet into the filter chamber: the structure, the opening angle shape;
4. The filter efficiency of the electric dust filter increases as the level of the air speed in the filter chamber improves, which means that the difference between the velocities is minimal.

CHAPTER 3: LABORATORY EQUIPMENT AND RESEARCH METHODS

3.1. Laboratory equipment

3.1.1. Experimental model

The model of dust filter is designed according to Russian standards with ratio (1:14) in comparison with reality

Figure 3.1. Physical model of electric dust filter for experiment

3.1.2. Measurement system of aerodynamic parameters

The instrumentation system of the aerodynamic physical model of the electrostatic precipitators includes, [57]:

To measure the aerodynamic parameters on the physical model P& ID diagram of Figure 3.2.

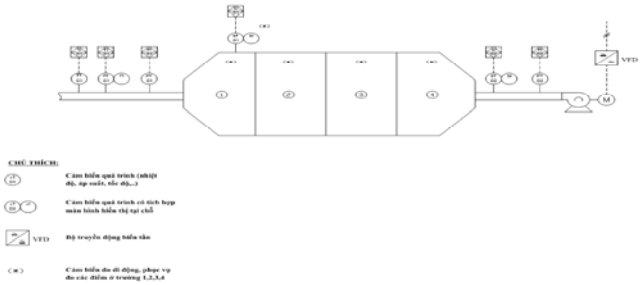

Figure 3.2. P & ID diagram of the experimental model

Figure 3.3. EE75 airflow speed meter,

3.1.2.1. EE75 airflow speed meter

Shown in Fig. 3.3

Operational principles:

Based on the principles of air flow measurement through hot wire, Elektronik has developed the E+E air speed sensor

3.1.2.2. Flow measurement device Proline T-mass B150

T Mass - B150 (fig. 3.6) is a device that can directly measure the volume of airflow in a convenient way. Output operation with many variables can measure the airflow, actual volume of airflow, volume of airflow FAD and thermodynamics.

Fig. 3.6. Flow measurement device Proline T-mass B150, [59]

1.2.3. Pressure measuring device Cerabar PMC131

Figure 3.10. Pressure measuring device Cerabar PMC13 Figure 3.12. Temperature measurement device TSM187

3.1.2.4. Temperature measurement device TSM187

Shown in fig. 3.12.

3.2. a) Arrangement of the measurement devices of aerodynamic parameters

3.2.1. Arrangement of the measurement chart of aerodynamic parameters of experimental model

a)

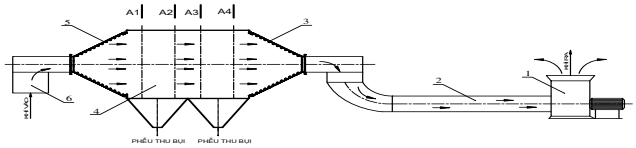

b)

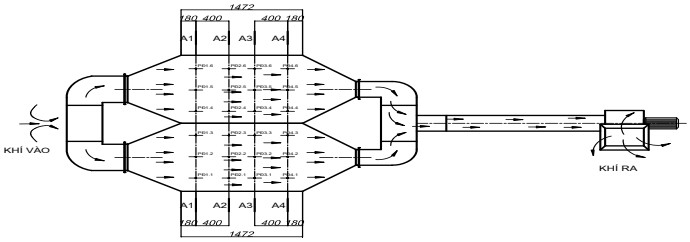

Figure 3.13. Diagram of aerodynamic speed measurement points on 4 sections in the model (24=4x6)
a) Arrangement of measurement points on 4 sections A_1 , A_2 ,A_3 and A_4 (vertical projection diagram); b) Arrangement of measurement points on 4 sections A1 , A2 ,A3 and A4 (projection diagram)

- *Description of the layout of airflow speed measurement*: Set the measurement point by 3x4 matrix. Set 16 special holes, divided into 4 rows, corresponding to 4 sections: A1, A2, A3 and A4.

- *How to use measurement diagram:* Place the measuring head in full 12 points, resulting in air speed displayed on the screen on each section: A1, A2, A3 and A4.

3.2.2. Flow measurement: use Proline T-mass B150 (fig. 3.6) and display directly on the screen.

3.2.3. Temperature measurement: use TSM187 and display directly on the screen.

3.2.4. Pressure measurement: use PMC131 and display directly on the screen. The input pressure of the electrostatic precipitators is set as the environmental pressure.

3.2.5. Some air speed standards

3.2.5.1. Standard for controlling uneven airflow speed

Standard ICAC-EP-7 is applied to check the distribution of the speed field in the electrostatic precipitator.

3.2.5.3. Uniform flow standard

In the near processing zone and the output of the electrostatic precipitator, the speed model must have a minimum of 85% of speed, no more than 1.15 times the average speed, and 99% of the speed does not exceed 1.40 times compared to the average speed.

3.3. Measuring instruments and airflow speed measurement process

3.3.1. Requirement of speedometer in laboratory

- Accurate and repeatable in about 2% of reading or 0.5% of scale;
- For electronic measuring equipment, there must be a system with a response time of less than 1 second.
- Systems (sensor, signal conditioning, data reading and writing) must be calibrated as often as required.

3.3.2. Requirements for speed measurement process for experimental and practical models

- There is a minimum number of test points equal to 1/9 of the cross-sectional area of the actual electrostatic precipitator surface, with at least three sections with multiple measurement points.;
- There are data taken near the leading edge of the first plate of the deposition electrodes and near the rear edge of the final plates of the deposition electrodes;
- It is possible to continuously record or measure discrete measurements taken and recorded using an automated data acquisition program.

3.4. Inspection and assembly of equipment

3.5. Selection of sampling locations

a) Sampling locations: Measurement of the airflow speed at the output and input of the electrostatic precipitator, the position after the first field, the second field.

b) Determining the number of sampling points: The minimum number of points defined can be used in table 3.1 to determine the number of sampling points.

Table 3.1: Matrix of sampling points for rectangular chimneys

Số điểm lấy mẫu	Ma trận
9	3 x 3
12	4 x 3
16	4 x 4
20	5 x 4
25	5 x 5
30	6 x 5
36	6 x 6
42	7 x 6
49	7 x 7

- 12 points for rectangular or circular chimney if D> 0.61m.
- 8 points for circular chimney if 0.3m <D <0.61m
- 9 points for rectangular chimney with 0.3 m <D <0.61 m

Thus, with the size of the cross-section at the rear of the first and second field, the number of the sampling point required would be 12 points:

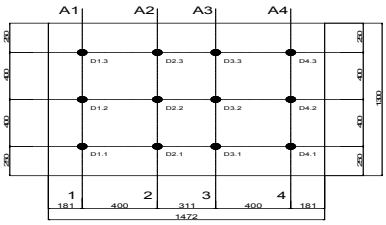

Figure 3.15. 12 sampling points on a section *Figure 3.16. Blower of the experimental model*

3.6. Airflow speed measurement method

3.6.2. Speed measurement method

The speed measurement process can use configuration software and procedure measurement using buttons on the control module (see steps in LA):

Blower: Technical characteristics of the blower in the model (figure 3.16):

+ Symbol: CPL3-6.31;+ Blower speed: 1450 rpm; blower performance: 22.000 m^3/h
+ Pressure column: 16.000 Pa; Capacity: 15kw

3.8. Installation location of air distribution plate

a) Installation at the input position:

12 positions to fit the flow distribution grille on the picture 3.17 (inlet is signed by V:V1 - V12), outlet is signed by R: R_1-R_{12}

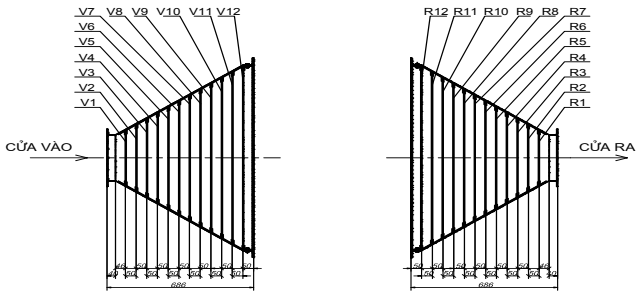

Figure 3.17. 12 positions of the flow distribution grille

3.12. Experimental options

3.12.1 Experimental objectives

Adjust the aerodynamic resistance by mechanical method is to adjust the grille position, the number of grille, the type of airflow distribution grille in the physical model filter chamber.

3.12.2 Theoretical basis for adjusting air resistance by airflow distribution grille

- *The screen has two basic effects:* The first is to divide the airflow into the filter chamber in order to focus on the effective space of the deposition plate system; the second is to make the level of the airflow speed field.

- One of the solutions to make the level of airflow speed is the use of serial installation of flow distribution grilles in the air channel [14, 16]. This is illustrated in Figure 3.19.

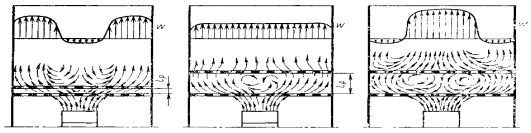

a) *b)* *c)*

Figure 3. 19. The speed field after the two flow distribution grilles with the ratio (l_p/ D_k) between the distance between them l_p and grille diameter D_k varies by 3 levels: a) Small L_p <0,05); b) reasonable L_p = (≈0,2), c) large L_p ($\zeta_p \geq \zeta_{kp}$)

- According to the author [14, 16] experiment on industrial electrostatic precipitators:

+ Option 1: There are 2 grilles with ventilation of: f = 45%; Option 2: There is 1 grille with ventilation reduced to f = 30%; Option 3: There is 1 grille with ventilation reduced to f = 22.5% ;

3.12.3. Experimental options

Option 1: No input and output grilles for both modules on the physical model. The purpose is to check the speed field condition in the filter chamber space when there is no flow distribution grille.

A. Square hole group

+ Option 2: Grille positions V_{10} and V_5 are fitted with the input and R_5 output for both modules on the physical model (Input V10:V5 => output R10:R5).

+ **Option 3:** Grille positions V_{10} and V_5 are fitted with the input and output for both modules on the physical model **(**Input V10:V5 => output R10).

+ **Option 4:** Grille position V_{10} is fitted with the input and 0 output for both modules on the physical model (Input V10 => output R10).

+ **Option 5:** Grille positions V_{10} and V_5 are fitted with the input and R_5 output for both modules on the physical model **(**Input V10:V5 => output R5).

+ **Option 6:** Grille positions V_{10} and V_5 are fitted with the input and none output for both modules on the physical model **(**Input V10:V5 => output 0).

B. Group of round hole options:

+ **Option 7:** Grille positions V_{10} and V_5 are fitted with the input and R_{10} output for both modules on the physical model **(**Input V10:V5 => output R10).

+ **Option 8:** Grille position V_{10} is fitted with the input and 0 output for both modules on the physical model (Input V10 => output R10).

Table 3.3: Measurement results of options

Measurement location	**Speed (m/s)**				**Remark**
	Section				
	1-1	2-2	3-3	4-4	
1	V_{11}	V_{21}	V_{31}	V_{41}	
2	V_{12}	V_{22}	V_{32}	V_{42}	
3	V_{13}	V_{23}	V_{33}	V_{43}	
4	V_{14}	V_{24}	V_{34}	V_{44}	
Average speed	$\mathbf{V_{TB14}}$	$\mathbf{V_{TB24}}$	$\mathbf{V_{TB\ 34}}$	$\mathbf{V_{TB44}}$	

3.13. Experimental data processing

To construct the equation from the experiment, it is necessary to linearize the nonlinear function:

Suppose the nonlinear function is a regression function of the form: $\tilde{y} = a.x^b$ (3.3)

Suppose $a > 0$ and $x > 0$, take the 10m logarithm of the two sides (3.3) we have:

$$\lg \tilde{y} = \lg a + b \lg x \quad (3.4)$$

Set new functions, new variables for (3.4): $Y = \lg \tilde{y}$; $A = \lg a$; $X = \lg x$

We obtain a new linear function: $\tilde{Y} = A + bX$ (3.5)

After finding the parameters A and b, we change under the original function: $\tilde{y} = 10^A x^b$ (3.6)

Calculating coefficients:

$$a_0 = \frac{\overline{y}.\overline{x^2} - \overline{x}.\overline{x.y}}{\overline{x^2} - \overline{(x)^2}} \quad (3.7)$$

$$a_1 = \frac{\overline{x.y} - \overline{x}.\overline{y}}{\overline{x^2} - \overline{(x)^2}} \quad (3.8)$$

Similar to the experimental values, get the parameters a_i and signed by $\hat{a}, \hat{a}_1$ and the correlation coefficient is:

$$S_x = \frac{\sum_{i=1}^{n} x_i^2 - n\overline{(x)^2}}{n-1}; \quad S_y = \frac{\sum_{i=1}^{n} y_i^2 - n\overline{(y)^2}}{n-1} \quad (3.9)$$

$$r_{xy} = \hat{a}_1 . \frac{S_x}{S_y} \quad (3.10)$$

The sum of squares is calculated as follows: $S_{(\hat{a}_0 + \hat{a}_1)} = (n-1) S_y^2 (1 - r_{xy})^2$ (3.11)

Criteria (3.9) and (3.10) to evaluate the experimental results.

Conclusion of chapter 3

1. Design and manufacture the physical model of electrostatic precipitator chamber, consisting of two fields connected with air inlet and outlet channel in rectangular from and blower with capacity of 22.000m^3/h, on the model, which is arranged 4 sections to install air speed measuring device;

2. A schematic diagram has been constructed at 4 sections on the filter chamber model to measure the speed field of a matrix of 12 points on each section and modern equipment to measure experimental parameters: air speed, air flow, speed measurement device connected to the result display;

3. 8 Experimental options have been selected, including 01 experimental option without flow distribution grille, 6 options with 9x9mm square hole grille and 2 options with round hole grille Φ10mm (details in 3.13.3).

4. Statistical methods were selected to analyze experimental data, to establish the relationship between the deviation of the speed field in the filter chamber and the measurement positions on each filter section at 12 measurement points.

CHAPTER 4: EXPERIMENTS, DATA PROCESSING, AND EVALUATION

The objective of the experiment: select fixed ventilation of 45% and opening angle of air channel select fixed 36^o. Accordingly, determine the level of speed field, select the most appropriate option with the best speed field.

4.1. Experimental conditions

Flow: Q_{sd} = 4000 m^3/h; Input air pressure, p = - 0,0KPa; air temperature in the filter chamber t = 28^{o}C; grille ventilation f=45%; grille from CT3 steel material, rectangular, hole of the flow distribution grille: square and round hole system; air environment without dust. Area of the filter chamber of the model: a x b = 1,156 x 1,186 = 1,37 m^2

Air speed in the filter chamber of the model: $v = \frac{Q_{sd}}{S} = \frac{4000}{3600.1,37} = 0,81$ m/s

4.2. Experimental description

a) Model structure:

b) Measurement scheme of parameters:

including: EE75 airflow speed sensor; Flow measurement sensor Proline T- mass B150; Pressure measurement sensor Cerabar PMC131;

- Temperature measurement sensor TSM187.

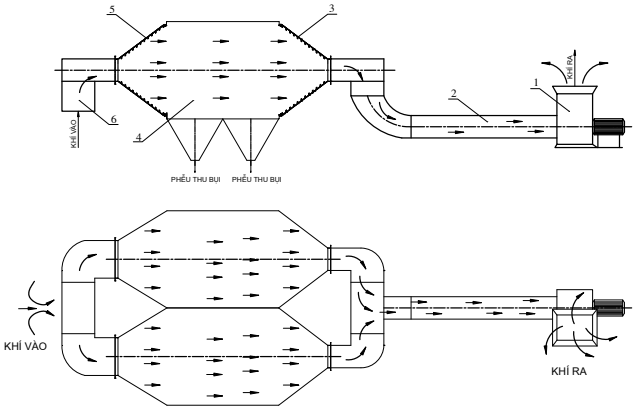

Figure 4.1. Diagram of electrostatic precipitator model

1. Exhaust fan; 2. Air conduit; 3. Door to install the flow distribution grille out; 4. Filter chamber; 5. Door to install the flow distribution grille in; 6. Air inlet

c) Methods of measuring parameters:

- Measurement of aerodynamic parameters of experimental model of electrostatic precipitator (H3.13);

- The air speed measured at 12 points (Table 3.17) is taken in the direction of the 4 cross-sections of the model. The results of the 4 options included in the table (4.1; 4.2; … 4.7).

4.3. Experimental results and experimental data processing

4.3.1 Experimental results

Experiment results are shown in the tables 4.1, 4.2, 4.3, 4.4, 4.5, 4.6, 4.7 and 4.8 corresponding to speed field diagrams of square holes of the figures: 4.2, 4.3, 4.4, 4.6 and 4.7.

Option 1: No grille for both input and output

Table 4.1a: Air speed measurement results in electrostatic precipitator model (no air distribution plate)

No.	Measuring point	Calculating speed	Section A1		Section A2		Section A3		Section A4	
			Actual speed (m/s)	Difference (%)	Actual speed (m/s)	Difference (%)	Actual speed (m/s)	Difference (%)	Actual speed . (m/s)	Difference (%)
1	P Đ1.1	0.81	0.4	-51%	0.3	-63%	0.3	-63%	0.5	-38%
2	P Đ1.2	0.81	0.2	-75%	0.4	-51%	0.1	-88%	0.4	-51%
3	P Đ1.3	0.81	0.3	-63%	0.4	-51%	0.1	-88%	0.3	-63%
4	P Đ1.4	0.81	0.3	-63%	0.3	-63%	0.1	-88%	0.4	-51%
			0.3	-63%	0.35	-57%	0.15	-81%	0.4	-51%
5	P Đ2.1	0.81	0.6	-26%	0.4	-51%	0.6	-26%	0.6	-26%
6	P Đ2.2	0.81	2.0	147%	2.7	233%	1.4	73%	1.0	23%
7	P Đ2.3	0.81	4.2	419%	2.1	159%	2.9	258%	2.8	246%
8	P Đ2.4	0.81	4.7	480%	0.7	-14%	3.9	381%	3.5	332%
			2.88	255%	1.475	82%	2.2	172%	1.98	144%
9	P Đ3.1	0.81	2.5	209%	2.7	233%	2	147%	2.0	147%
10	P Đ3.2	0.81	2.1	159%	2.1	159%	2.8	246%	2.2	172%
11	P Đ3.3	0.81	1.2	48%	1.5	85%	1.4	73%	1.2	48%
12	P Đ3.4	0.81	0.9	11%	0.7	-14%	1.7	110%	0.9	11%
			1.68	107%	1.75	116%	1.975	144%	1.58	94%

Table 4.1b: Calculation result of the average air speed in the electrostatic precipitator model (no air distribution plate)

No.	Measuring point	Calculating speed	Section A1		Section A2		Section A3		Section A4	
			Actual speed (m/s)	Difference (%)	Actual speed (m/s)	Difference (%)	Actual speed (m/s)	Difference (%)	Actual speed . (m/s)	Difference (%)
1	P Đ1	0.81	0.3	-63%	0.35	-57%	0.15	-81%	0.4	-51%
2	P Đ2	0.81	2.88	255%	1.48	82%	2.20	172%	1.98	144%
3	P Đ3	0.81	1.68	107%	1.75	116%	1.98	144%	1.58	94%

Experiment parameter: F = 35Hz; Open door 1/2; $V_{1(input)}$= 6,2m/s; $V_{2(output)}$= 11.6m/s

$P_{1(input)}$= -0,4kpa; $P_{2(output)}$= -0.13kpa; H = 813m^3/h

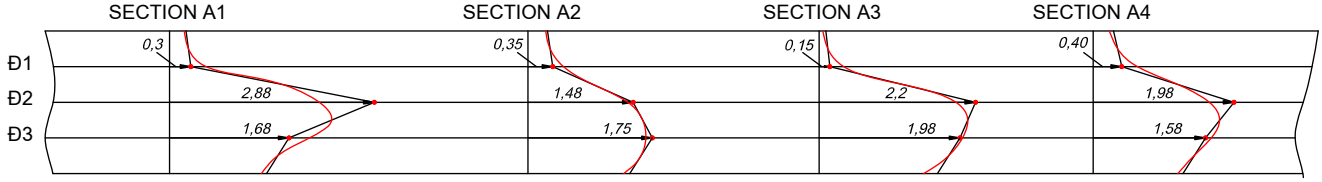

Figure 4.2b. Speed in Table 4.1b measured at 6 points, 4 sections: A1, A2, A3, A4

Comment on the results of the option 1 without grille: Experimental results show that the maximum difference is 207% and the minimum one is 12%.

I. Square hole system options

Option 2: (Input V10:V5 => output R10:R5)

Table 4.2a: Air speed measurement results in the dust filter model (Input V5:V10=> output R10:R5)

No.	Measuring point	Calculating speed	Section A1		Section A2		Section A3		Section A4	
			Actual speed (m/s)	Difference (%)	Actual speed (m/s)	Difference (%)	Actual speed (m/s)	Difference (%)	Actual speed . (m/s)	Difference (%)
1	P Đ1.1	0.81	0.7	-14%	0.8	-1%	0.8	-1%	0.9	11%
2	P Đ1.2	0.81	0.7	-14%	0.8	-1%	0.8	-1%	0.9	11%
3	P Đ1.3	0.81	0.7	-14%	0.8	-1%	0.8	-1%	0.9	11%
4	P Đ1.4	0.81	0.7	-14%	0.8	-1%	0.8	-1%	1	23%
			0.7	-14%	0.8	-1%	0.8	-1%	0.925	14%
5	P Đ2.1	0.81	0.8	-1%	0.7	-14%	0.9	11%	0.9	11%
6	P Đ2.2	0.81	0.7	-14%	0.6	-26%	0.7	-14%	0.9	11%
7	P Đ2.3	0.81	0.8	-1%	0.6	-26%	0.7	-14%	0.9	11%
8	P Đ2.4	0.81	0.7	-14%	0.7	-14%	0.8	-1%	0.9	11%
			0.75	-7%	0.65	-20%	0.775	-4%	0.9	11%
9	P Đ3.1	0.81	0.7	-14%	0.8	-1%	0.9	11%	1.1	36%
10	P Đ3.2	0.81	0.7	-14%	0.7	-14%	0.7	-14%	0.9	11%
11	P Đ3.3	0.81	0.7	-14%	0.9	11%	0.9	11%	0.8	-1%
12	P Đ3.4	0.81	0.8	-1%	0.8	-1%	0.8	-1%	0.9	11%
			0.725	-10%	0.8	-1%	0.825	2%	0.925	14%

Table 4.2b: Calculation results of the average air speed in the electrostatic precipitator model (Input V5:V10 => output R5:R10

No.	Measuring point	Calculating speed	Section A1		Section A2		Section A3		Section A4	
			Actual speed (m/s)	Difference (%)	Actual speed (m/s)	Difference (%)	Actual speed (m/s)	Difference (%)	Actual speed . (m/s)	Difference (%)
1	P Đ1	0.81	0.7	-14%	0.8	-1%	0.8	-1%	0.925	14%
2	P Đ2	0.81	0.75	-7%	0.65	-20%	0.775	-4%	0.9	11%
3	P Đ3	0.81	0.725	-10%	0.8	-1%	0.825	2%	0.925	14%

Experiment parameters: F = 35Hz; Open door 1/2; $V_{1(input)}$= 6,2m/s; $V_{2(output)}$= 13m/s

$P_{1(input)}$= -0,05kpa; $P_{2(output)}$= -0.16kpa; H = 805m^3

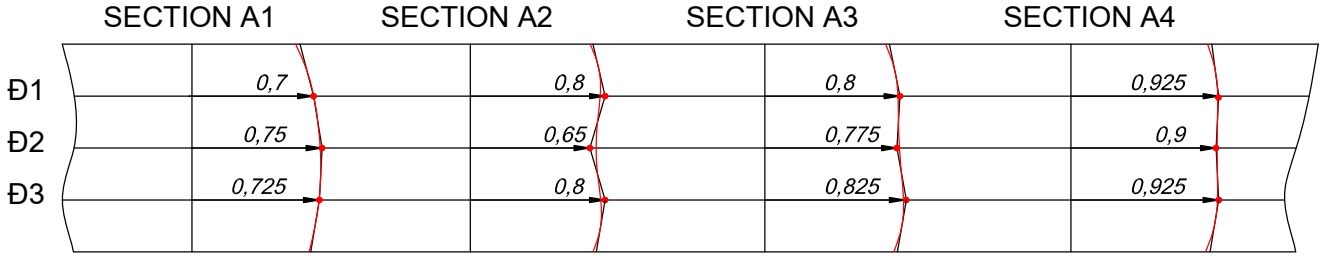

Figure 4.3b. Speed in table 4.2 measured at 3 points, 4 sections: A_1, A_2, A_3, A_4

Comment on the results of option 2: Experimental results show that the maximum difference is 19% and the minimum one is 3%.

Option 3: Input V10:V5 => output R10

Table 4.3a: Air speed measurement results in the dust filter model with spare hole air distribution plate (input V10:V5 => output R10)

No.	Measuring point	Calculating speed	Section A1		Section A2		Section A3		Section A4	
			Actual speed (m/s)	Difference (%)	Actual speed (m/s)	Difference (%)	Actual speed (m/s)	Difference (%)	Actual speed . (m/s)	Difference (%)
1	P Đ1.1	0.81	0.7	-14%	0.8	-1%	0.9	11%	1.1	36%
2	P Đ1.2	0.81	0.7	-14%	0.8	-1%	0.9	11%	0.9	11%
3	P Đ1.3	0.81	0.8	-1%	0.8	-1%	0.8	-1%	0.9	11%
4	P Đ1.4	0.81	0.7	-14%	0.8	-1%	0.8	-1%	0.9	11%
			0.725	-10%	0.8	-1%	0.85	5%	0.95	17%
5	P Đ2.1	0.81	0.7	-14%	0.7	-14%	0.9	11%	0.9	11%
6	P Đ2.2	0.81	0.7	-14%	0.6	-26%	0.7	-14%	0.8	-1%
7	P Đ2.3	0.81	0.6	-26%	0.6	-26%	0.6	-26%	0.8	-1%
8	P Đ2.4	0.81	0.7	-14%	0.7	-14%	0.8	-1%	0.9	11%
			0.675	-17%	0.65	-20%	0.75	-7%	0.85	5%
9	P Đ3.1	0.81	0.9	11%	0.9	11%	1.1	36%	1.1	36%
10	P Đ3.2	0.81	0.9	11%	0.8	-1%	0.9	11%	0.9	11%
11	P Đ3.3	0.81	0.8	-1%	0.7	-14%	1	23%	0.8	-1%
12	P Đ3.4	0.81	0.9	11%	0.7	-14%	0.9	11%	0.9	11%
			0.875	8%	0.775	-4%	0.975	20%	0.925	14%

Table 4.3b: Average air speed measurement results in the dust filter with square hole air distribution plate (Input V5:V10 => Output R10)

No.	Measuring point	Calculating speed	Section A1		Section A2		Section A3		Section A4	
			Actual speed (m/s)	Difference (%)	Actual speed (m/s)	Difference (%)	Actual speed (m/s)	Difference (%)	Actual speed . (m/s)	Difference (%)
1	P Đ1	0.81	0.725	-10%	0.8	-1%	0.85	5%	0.95	17%
2	P Đ2	0.81	0.675	-17%	0.65	-20%	0.75	-7%	0.85	5%
3	P Đ3	0.81	0.875	8%	0.775	-4%	0.975	20%	0.925	14%

Experiment parameters: F = 35Hz; Open door 1/2; $V_{1(input)}$= 6,6m/s; $V_{2(output)}$= 11.76m/s

$P_{1(input)}$= -0,04kpa; $P_{2(output)}$= -0.15kpa; H = 711m^3/h

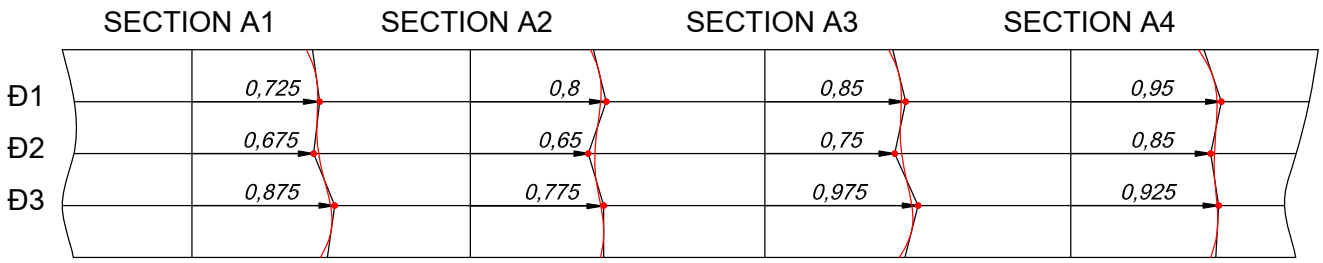

Figure 4.4b. Speed in table 4.3b measured at 3 points, 4 sections: A_1, A_2, A_3, A_4

Comment on the results of option 3: Experimental results show the maximum difference of 19% and minimum one of 6%.

Option 4: (Input V10 => output R10)

Table 4.4a: Air speed measurement results in the dust filter with square hole air distribution plate (Input V10 => Output R10)

No.	Measuring point	Calculating speed	Section A1		Section A2		Section A3		Section A4	
			Actual speed (m/s)	Difference (%)	Actual speed (m/s)	Difference (%)	Actual speed (m/s)	Difference (%)	Actual speed . (m/s)	Difference (%)
1	P Đ1 1	0.81	0.6	-26%	0.6	-26%	0.8	-1%	0.8	-1%
2	P Đ1 2	0.81	0.5	-38%	0.6	-26%	0.7	-14%	0.9	11%
3	P Đ1 3	0.81	0.6	-26%	0.7	-14%	0.8	-1%	0.9	11%
4	P Đ1 4	0.81	0.6	-26%	0.7	-14%	0.9	11%	1	23%
			0.575	-29%	0.65	-20%	0.8	-1%	0.9	11%
5	P Đ2 1	0.81	0.5	-38%	0.6	-26%	0.9	11%	0.9	11%
6	P Đ2 2	0.81	0.6	-26%	0.6	-26%	0.7	-14%	0.8	-1%
7	P Đ2 3	0.81	0.7	-14%	0.7	-14%	0.7	-14%	0.9	11%
8	P Đ2 4	0.81	0.6	-26%	0.7	-14%	0.8	-1%	0.9	11%
			0.6	-26%	0.65	-20%	0.775	-4%	0.875	8%
9	P Đ3 1	0.81	0.6	-26%	0.7	-14%	0.8	-1%	1	23%
10	P Đ3 2	0.81	0.7	-14%	0.8	-1%	0.7	-14%	0.8	-1%
11	P Đ3 3	0.81	0.7	-14%	0.8	-1%	0.8	-1%	0.9	11%
12	P Đ3 4	0.81	0.7	-14%	0.8	-1%	0.9	11%	0.9	11%
			0.675	-17%	0.775	-4%	0.8	-1%	0.9	11%

Table 4.4b: Average air speed measurement results in the dust filter with square hole air distribution plate (Input V10 => Output R10)

No.	Measuring point	Calculating speed	Section A1		Section A2		Section A3		Section A4	
			Actual speed (m/s)	Difference (%)	Actual speed (m/s)	Difference (%)	Actual speed (m/s)	Difference (%)	Actual speed . (m/s)	Difference (%)
1	P Đ1	0.81	0.575	-29%	0.65	-20%	0.8	-1%	0.9	11%
2	P Đ2	0.81	0.6	-26%	0.65	-20%	0.775	-4%	0.875	8%
3	P Đ3	0.81	0.675	-17%	0.775	-4%	0.80	-1%	0.90	11%

Experiment parameters: F = 35Hz; Open door 1/2; $V_{1(input)}$= 6,4m/s; $V_{2(output)}$= 11.4m

$P_{1(input)}$= -0,05kpa; $P_{2(output)}$= -0.14kpa; H = 755m^3/h;

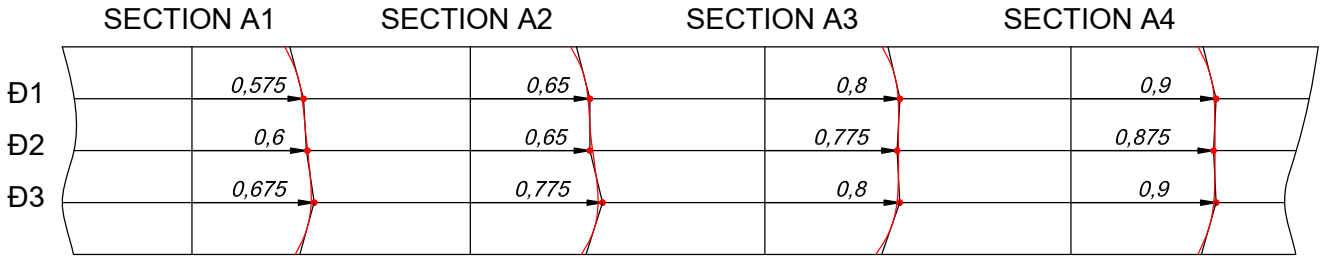

Figure 4.5b. Speed in table 4.4b measured at 3 points, 4 sections: A_1, A_2, A_3, A_4

Comment on the results of option 4: Experimental results show the maximum difference of 16% and minimum one of 3%.

Option 5: Input V10:V5 => output R5

Table 4.5a: Air speed measurement results in the dust filter model with square hole air distribution plate (Input V10:V5 => Output R5)

No.	Measuring point	Calculating speed	Section A1		Section A2		Section A3		Section A4	
			Actual speed (m/s)	Difference (%)	Actual speed (m/s)	Difference (%)	Actual speed (m/s)	Difference (%)	Actual speed . (m/s)	Difference (%)
1	P Đ1.1	0.81	0.6	-26%	0.8	-1%	0.9	11%	0.9	11%
2	P Đ1.2	0.81	0.7	-14%	0.8	-1%	0.8	-1%	0.9	11%
3	P Đ1.3	0.81	0.7	-14%	0.7	-14%	0.8	-1%	0.9	11%
4	P Đ1.4	0.81	0.7	-14%	0.7	-14%	0.9	11%	0.8	-1%
			0.675	-17%	0.75	-7%	0.85	5%	0.875	8%
5	P Đ2.1	0.81	0.7	-14%	0.7	-14%	0.8	-1%	0.9	11%
6	P Đ2.2	0.81	0.6	-26%	0.6	-26%	0.7	-14%	0.8	-1%
7	P Đ2.3	0.81	0.6	-26%	0.7	-14%	0.7	-14%	0.9	11%
8	P Đ2.4	0.81	0.7	-14%	0.8	-1%	0.8	-1%	0.9	11%
			0.65	-20%	0.7	-14%	0.75	-7%	0.875	8%
9	P Đ3.1	0.81	0.8	-1%	0.8	-1%	0.8	-1%	0.8	-1%
10	P Đ3.2	0.81	0.8	-1%	0.7	-14%	0.9	11%	0.8	-1%
11	P Đ3.3	0.81	0.7	-14%	0.7	-14%	0.7	-14%	0.9	11%
12	P Đ3.4	0.81	0.8	-1%	0.8	-1%	0.8	-1%	0.9	11%
			0.775	-4%	0.75	-7%	0.8	-1%	0.85	5%

Table 4.5b: Average air speed measurement results in the dust filter with square hole air distribution plate (Input V5:V10 => Output R5)

No.	Measuring point	Calculating speed	Section A1		Section A2		Section A3		Section A4	
			Actual speed (m/s)	Difference (%)	Actual speed (m/s)	Difference (%)	Actual speed (m/s)	Difference (%)	Actual speed . (m/s)	Difference (%)
1	P Đ1	0.31	0.675	-17%	0.75	-7%	0.85	5%	0.875	8%
2	P Đ2	0.31	0.65	-20%	0.70	-14%	0.75	-7%	0.875	8%
3	P Đ3	0.31	0.775	-4%	0.75	-7%	0.80	-1%	0.85	5%

Experiment parameters: F = 35Hz; Open door 1/2; $V_{1(input)}$= 6,3m/s; $V_{2(output)}$= 12,1m/s
$P_{1(input)}$= -0,06kpa; $P_{2(output)}$= -0.17kpa; H = 790m^3/h

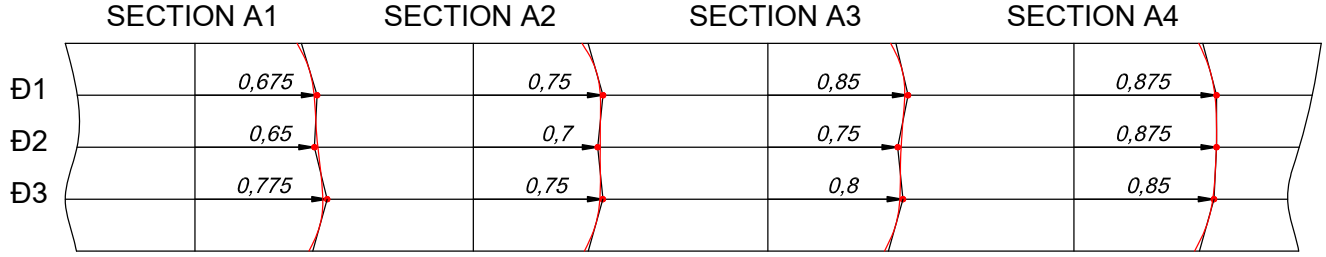

Figure 4.6b Speed in table 4.5b measured at 3 points, 4 sections: A_1, A_2, A_3, A_4

Comment on the results of option 5: Experimental results show the maximum difference of 25% and minimum one of 3%.

Option 6: Input V10:V5 => output without grille

Table 4.6a: Air speed measurement results in the dust filter model with square hole air distribution plate (Input V10:V5 => Output 0)

No.	Measuring point	Calculating speed	Section A1		Section A2		Section A3		Section A4	
			Actual speed (m/s)	Difference (%)	Actual speed (m/s)	Difference (%)	Actual speed (m/s)	Difference (%)	Actual speed . (m/s)	Difference (%)
1	P Đ1.1	0.81	0.5	-38%	0.7	-14%	0.8	-1%	0.8	-1%
2	P Đ1.2	0.81	0.7	-14%	0.7	-14%	0.8	-1%	0.8	-1%
3	P Đ1.3	0.81	0.6	-26%	0.6	-26%	0.7	-14%	0.9	11%
4	P Đ1.4	0.81	0.6	-26%	0.7	-14%	0.9	11%	0.9	11%
			0.6	-26%	0.675	-17%	0.8	-1%	0.85	5%
5	P Đ2.1	0.81	0.8	-1%	0.8	-1%	0.8	-1%	0.9	11%
6	P Đ2.2	0.81	0.5	-38%	0.7	-14%	0.8	-1%	0.7	-14%
7	P Đ2.3	0.81	0.6	-26%	0.7	-14%	0.7	-14%	0.8	-1%
8	P Đ2.4	0.81	0.7	-14%	0.5	-38%	0.8	-1%	0.9	11%
			0.65	-20%	0.675	-17%	0.775	-4%	0.825	2%
9	P Đ3.1	0.81	0.8	-1%	0.7	-14%	0.8	-1%	0.9	11%
10	P Đ3.2	0.81	0.6	-26%	0.8	-1%	0.9	11%	0.8	-1%
11	P Đ3.3	0.81	0.5	-38%	0.8	-1%	0.7	-14%	0.9	11%
12	P Đ3.4	0.81	0.8	-1%	0.7	-14%	0.9	11%	1	23%
			0.675	-17%	0.75	-7%	0.825	2%	0.9	11%

Table 4.6b: Average air speed measurement results in the dust filter with square hole air distribution plate (Input V5:V10 => Output 0)

No.	Measuring point	Calculating speed	Section A1		Section A2		Section A3		Section A4	
			Actual speed (m/s)	Difference (%)	Actual speed (m/s)	Difference (%)	Actual speed (m/s)	Difference (%)	Actual speed . (m/s)	Difference (%)
1	P Đ1	0.81	0.6	-26%	0.675	-17%	0.8	-1%	0.85	5%
2	P Đ2	0.81	0.65	-20%	0.675	-17%	0.775	-4%	0.825	2%
3	P Đ3	0.81	0.675	-17%	0.75	-7%	0.825	2%	0.90	11%

Experiment parameters: F = 35Hz; Open door 1/2; $V_{1(input)}$= 6,2m/s; $V_{2(output)}$= 11.5m/s
$P_{1(input)}$= -0,04kpa; $P_{2(output)}$= -0.15kpa; H = 789m^3/h

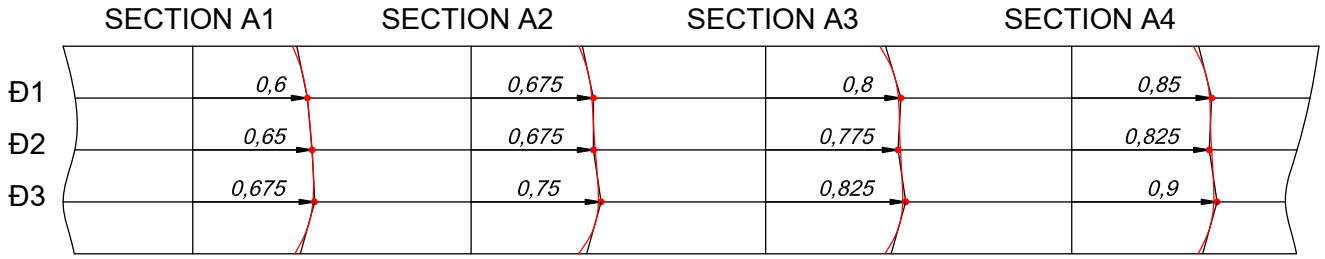

Figure 4.7b. Speed in table 4.6b measured at 3 points, 4 sections: A_1, A_2, A_3, A_4

Comment on the results of option 6: Experimental results show the maximum difference of 25% and minimum one of 3%.

II. Round hole option

Option 7a: Installation of 2 round hole grilles with input V10:V5 output R10

Table 4.7a: Air speed measurement results in the dust filter model with round hole air distribution plate (Input V5:V10 => Output R10)

No.	Measuring point	Calculating speed	Section A1		Section A2		Section A3		Section A4	
			Actual speed (m/s)	Difference (%)	Actual speed (m/s)	Difference (%)	Actual speed (m/s)	Difference (%)	Actual speed . (m/s)	Difference (%)
1	P Đ1.1	1.0	0.9	-11%	0.8	-21%	0.8	-21%	0.9	-11%
2	P Đ1.2	1.0	0.8	-21%	0.8	-21%	0.9	-11%	0.9	-11%
3	P Đ1.3	1.0	0.8	-21%	0.7	-31%	0.9	-11%	0.9	-11%
4	P Đ1.4	1.0	0.8	-21%	0.8	-21%	0.8	-21%	0.9	-11%
			0.825	-18%	0.775	-23%	0.85	-16%	0.9	-11%
5	P Đ2.1	1.0	0.8	-21%	0.8	-21%	0.9	-11%	1.1	9%
6	P Đ2.2	1.0	0.8	-21%	0.7	-31%	0.8	-21%	0.9	-11%
7	P Đ2.3	1.0	0.8	-21%	0.7	-31%	0.7	-31%	0.9	-11%
8	P Đ2.4	1.0	0.7	-31%	0.8	-21%	0.9	-11%	0.9	-11%
			0.775	-23%	0.75	-28%	0.825	-18%	0.95	-6%
9	P Đ3.1	1.0	0.9	-11%	0.9	-11%	1	-1%	1	-1%
10	P Đ3.2	1.0	0.9	-11%	0.9	-11%	0.9	-11%	1	-1%
11	P Đ3.3	1.0	0.9	-11%	0.8	-21%	0.8	-21%	0.9	-11%
12	P Đ3.4	1.0	0.9	-11%	0.8	-21%	0.8	-21%	0.9	-11%
			0.9	-11%	0.85	-18%	0.875	-13%	0.95	-6%

Table 4.7b: Average air speed measurement results in the dust filter with round hole air distribution plate (Input V5:V10 => Output R10)

No.	Measuring point	Calculating speed	Section A1		Section A2		Section A3		Section A4	
			Actual speed (m/s)	Difference (%)	Actual speed (m/s)	Difference (%)	Actual speed (m/s)	Difference (%)	Actual speed . (m/s)	Difference (%)
1	P Đ1	0.81	0.825	-18%	0.775	-23%	0.85	-16%	0.9	-11%
2	P Đ2	0.81	0.775	-23%	0.75	-26%	0.825	-18%	0.95	-6%
3	P Đ3	0.81	0.90	-11%	0.85	-16%	0.875	-13%	0.95	-6%

Experiment parameters: F = 35Hz; Open door 1/2; $V_{1(input)}$= 6,0m/s; $V_{2(output)}$= 12,2m/s
$P_{1(input)}$= -0,02kpa; $P_{2(output)}$= -0.11kpa; H = 798m^3/h

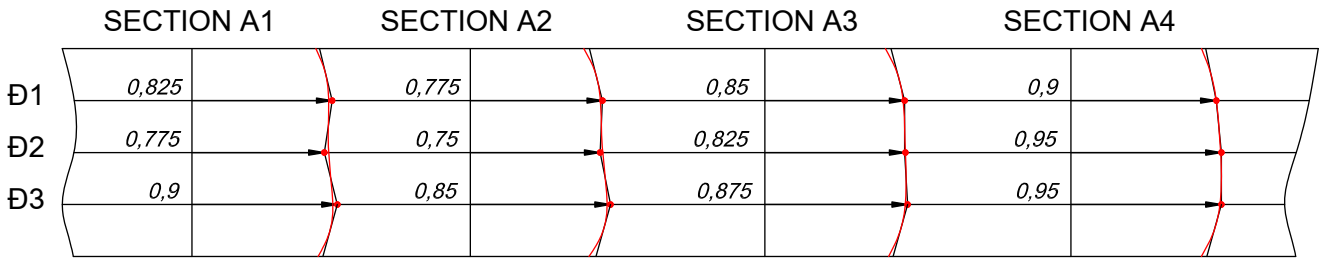

Figure 4.8b. Speed in table 4.7b at 3 points, 4 sections: I, II, III, IV corresponding measurement positions of the square hole at A_1, A_2, A_3, A_4

Comment on the results of option 7 (Round hole): Experimental results show the maximum difference of 17% and minimum one of 5%.

Option 8: Installation of round hole grille (Input V10 => output R10)

Table 4.8a: Air speed measurement results in the dust filter model with round hole air distribution plate (Input V10 => Output R10)

No.	Measuring point	Calculating speed	Section A1		Section A2		Section A3		Section A4	
			Actual speed (m/s)	Difference (%)	Actual speed (m/s)	Difference (%)	Actual speed (m/s)	Difference (%)	Actual speed . (m/s)	Difference (%)
1	P Đ1.1	0.81	0.7	-14%	0.8	-1%	0.8	-1%	0.8	-1%
2	P Đ1.2	0.81	0.7	-14%	0.8	-1%	0.8	-1%	0.8	-1%
3	P Đ1.3	0.81	0.7	-14%	0.8	-1%	0.8	-1%	0.8	-1%
4	P Đ1.4	0.81	0.7	-14%	0.8	-1%	0.8	-1%	0.9	11%
			0.7	-14%	0.8	-1%	0.8	-1%	0.825	2%
5	P Đ2.1	0.81	0.8	-1%	0.7	-14%	0.7	-14%	0.9	11%
6	P Đ2.2	0.81	0.7	-14%	0.7	-14%	0.7	-14%	0.9	11%
7	P Đ2.3	0.81	0.8	-1%	0.7	-14%	0.7	-14%	0.9	11%
8	P Đ2.4	0.81	0.7	-14%	0.7	-14%	0.7	-14%	0.9	11%
			0.75	-7%	0.7	-14%	0.7	-14%	0.9	11%
9	P Đ3.1	0.81	0.7	-14%	0.7	-14%	0.7	-14%	0.8	-1%
10	P Đ3.2	0.81	0.7	-14%	0.7	-14%	0.8	-1%	0.9	11%
11	P Đ3.3	0.81	0.7	-14%	0.6	-26%	0.7	-14%	0.9	11%
12	P Đ3.4	0.81	0.8	-1%	0.8	-1%	0.7	-14%	0.9	11%
			0.725	-10%	0.7	-14%	0.725	-10%	0.875	8%

Table 4.8b: Average air speed measurement results in the dust filter with round hole air distribution plate (Input V10 => Output R10)

No.	Measuring point	Calculating speed	Section A1		Section A2		Section A3		Section A4	
			Actual speed (m/s)	Difference (%)	Actual speed (m/s)	Difference (%)	Actual speed (m/s)	Difference (%)	Actual speed . (m/s)	Difference (%)
1	P Đ1	0.81	0.7	-14%	0.8	-1%	0.8	-1%	0.825	2%
2	P Đ2	0.81	0.75	-7%	0.7	-14%	0.7	-14%	0.9	11%
3	P Đ3	0.81	0.725	-10%	0.7	-14%	0.725	-10%	0.875	8%

Experiment parameters: F = 35Hz; Open door 1/2; $V_{1(input)}$= 6,2m/s; $V_{2(output)}$= 12.2m/s
$P_{1(input)}$= -0,03kpa; $P_{2(output)}$= -0.13kpa; H = 775m^3/h;

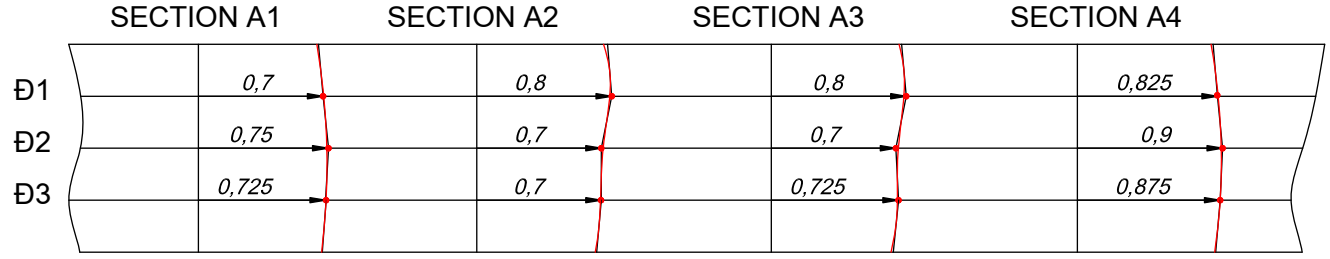

Figure 4.9b. Speed in table 4.8b at 3 points, 4 sections: I, II, III, IV corresponding measurement positions of the square hole at A_1, A_2, A_3, A_4

Comment on the results of option 8 (Round hole): Experimental results show the maximum difference of 13% and minimum one of 3%.

Comment on experiment results

- *The method of no installation of flow distribution grille*: no distribution grille, the variable speed varies on all four sections A1, A2, A3, A4.

- *When there is a flow divider*: When there is a flow distribution grille, the difference in speed on the same section is small. [7].

- *When the flow distribution* grille is not asymmetrical in quantity: In this case, the difference in speed increases. [7], [8], [9];

- *When symmetric installation of flow distribution grille*: The difference in speed is quite small when the grille is symmetric when installing 01 **input grille and 01 output grille** [7], [8], [9];

- With the grille clearance coefficient (45%) when grille installed is equal in number, the hole system has a difference in speed less than square hole system. Therefore, the square hole grille, when machined to round the corners to reduce the influence of air speed level;

- The grille installation method has reached a uniform parity of 10-20%. This opens up the possibility of diversifying the use of electric distribution grilles into electric precipitators in Vietnam, to overcome dependence on circular holes, which cost about 60% more.

4.4. Experiment data processing

4.4.1. Linearization of nonlinear functions

- Select the test result of each cross section at the center to determine the test result at 12 points = 3x4 (taken from the mean value at each measurement point xi, corresponding to the value of the error yi);

- Calculate the total and average values in tables p2, p3, p4, p5, p6, p7 and p8 of options 2, 3, 4, 5, 6, 7 and 8;

4.4.2. Evaluate the speed error from experiment results

To evaluate the air speed level based on experiment results, the difference in speed of two alternatives (square hole) and plan 8 (round hole) should be considered. Figure 4.10 shows the difference in speed of 2nd option (square hole system) and in Figure 4.11 is that of the 8th option (circular hole system):

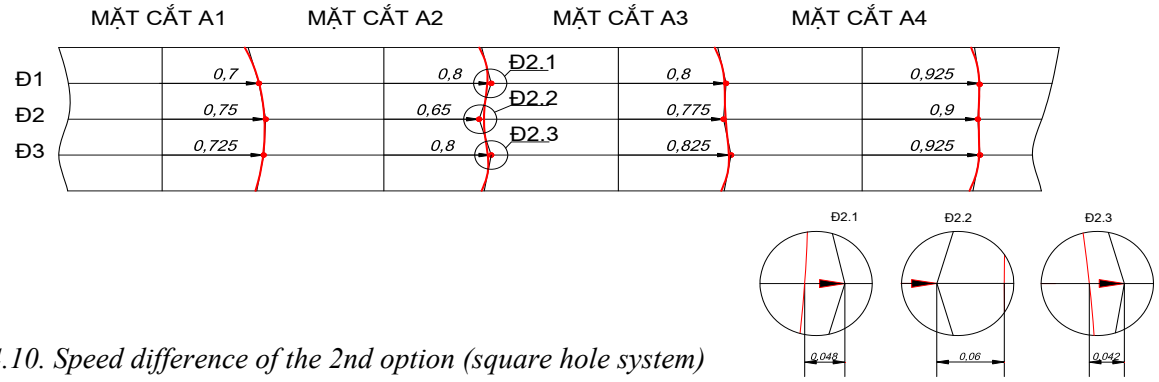

Figure 4.10. Speed difference of the 2nd option (square hole system)

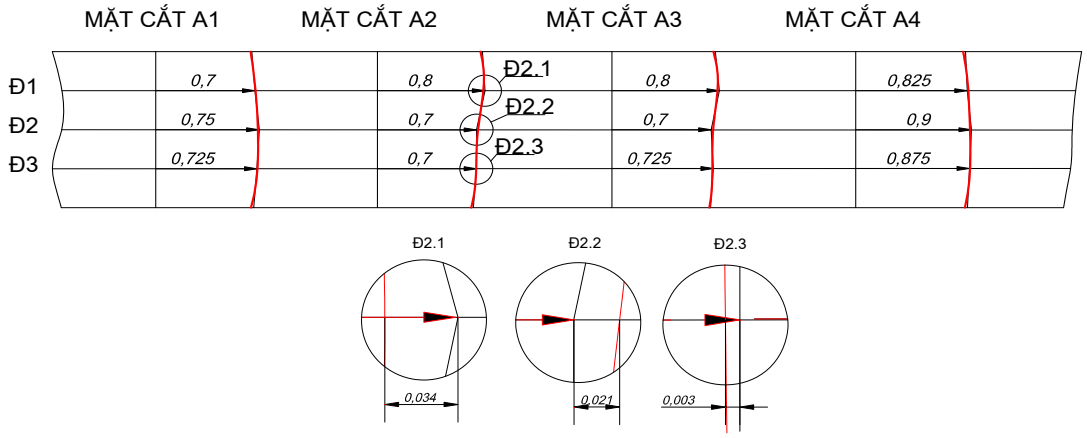

Figure 4.11. Speed difference of the 2nd option (circular hole system)

Comment on experiment data processing results:

- The results of the rationality test of the experimental regression equation show that the speed field is equal to the allowable speed, ie, the graph of the equation corresponds to the experiment points;
- The actual measurement results of the speed difference in the plot of the 2nd option (square hole) and the 8th option (circular hole) in Figures 10 and 11 are very small compared to the theory.

4.4.3. Make 3D graphs

Based on the real regression equation, make 3D graphs for alternatives: 2, 3, 4, 5, 6, 7, and 8, corresponding to the options in the following P2 - P8:

Option 2: Square hole (Input V10: V5 => Output R10: R5)

Shown in Figure 4.12.

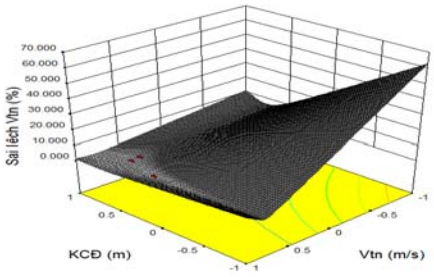

Figure 4.12.

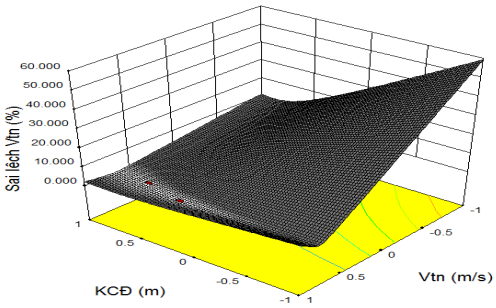

Figure 4.18.

The 8th option: Round hole (Input V10 => Output R10)

Shown in Figure 1.8

4.5. Test results on industrial static precipitator

4.5.1. Overview of precipitator at Cao Ngan thermal power plant

The 55 MW Q/2DC-31 industrial electrostatic precipitator is shown in Figure 4.9

4.5.2. Application of experimental results on test model into industrial precipitator

Step 1: Installation of the grille and test run sequence

1) Inspection:

2) Selection of grille suitable for grille was tested on the model:

The grille selection obtained the same grille specifications on the V10 input and R10 output models (hole D10).

- Grille shape is rectangular; The grille hole is round;
- The method of arranging the hole in the concentric circle with the position of the holes of two adjacent loops is staggered; Installation position of the line at the entrance and exit are equivalent;
- Diameter of holes compared to holes in the grille of the experimental model at 1:10. Specific holes on the Experimental Grille on industrial equipment models are D100 (V10 and R10) fitting symmetrically for input and output gates; - Open air is 45%.

3) Adjust the door towards the center of the filter chamber:

4) Technical cleaning; 5) start the idle equipment without load; 6) Run the machine at load; 7) Measure experimental data:

Check the technical parameters of the device: air flow, air speed, dust content at the input and output of the device, check filter performance.

8) Experimental data processing:

Calculate filter efficiency for alternatives based on dust content at the input and output parameters. Experiment results are recorded in Table 4.8

9) Evaluation of experimental results:

Table 4.8: Experimental results of uniform speed field using the experimental results of fitting a symmetrical V100 and R100 array on a 55MW electric precipitator

Table 4.8: Experimental results of the speed level using the experimental results of fitting a symmetrical V100 and R100 array on a 55 MW electric precipitator

Types of flow distribution grille	Average dust content			Air speed (m/s)		Performance(%)	
	Input filter chamber (g/ Nm^3)	Chimney outlet					
		Before application (mg/Nm^3)	After application (mg/Nm^3)	Input	Output	Prior to the application of the distribution grille	After to the application of the distribution grille
Circular hole grille system: - Input grille V100- Output grille R100	40	180	90	6	**11**	**98,1**	**99,2**

Comment: Dust extraction performance is 1.1% higher than before: 99.2-98.1 = 1.1%

4.6. Discuss the scientific results of the thesis

- *The method of no installation of flow distribution grille*: no distribution grille, the variable speed varies on all four sections A1, A2, A3, A4.

- *When there is a flow divider*: When there is a flow distribution grille, the difference in speed on the same section is small. [7].

- *When the flow distribution* grille is not asymmetrical in quantity: In this case, the difference in speed increases. [7], [8], [9];

- *When symmetric installation of flow distribution grille*: The difference in speed is quite small when the grille is symmetric when installing 01 **input grille and 01 output grille** [7], [8], [9];

- *Comparison of two types of grille:* With the coefficient of grille open constant (45%) when the grille is equal in number, the circular hole has a difference in speed less than square hole. This can be explained by the fact that round holes have no angles, with little change in the characteristics of the flow of air relative to square holes. Therefore, the square hole grille, when machined to round the corners to reduce the influence of air speed level;

- *The ability to apply square grille system in practice:* The square grille system has reached equalized (deviation) from 12 - 17%. This opens up the possibility of diversifying the use of electric distribution grilles into electric precipitators in Vietnam, around the dependence on circular holes, which costs about 60% more. [6].

Conclusion of Chapter 4

- Option 1: flow distribution grille: speed is very different on all four sections A1, A2, A3, A4;

- The mathematical relationship between the air speed error and the measurement location distance on a filter section was developed. This allows the assessment of the uniformity of the velocities at different measurement points on the same cross section;

- The results of calculating the condition coefficient of the experimental regression equations show: $r_{xy} = \hat{a}_1 . \frac{S_x}{S_y}$ and total residual squared $S_{(\hat{a}_0+\hat{a}_1)} = (n-1)S_y^2(1-r_{xy})^2$ qualified. This indicates the uniformity of the speed field in the filter chamber.

- Option 2: In case of installing 2 square grille system at the entrance and exit, the difference in speed on the same section is quite small (7-17%);

- The 7th option 7: Put the grille into V10 to R10 hole system, the difference in speed on the same section is very small (3 - 13%) on 4 sections;

- With the coefficient of ventilation (45%) of the grille when the grille is equal in number, the circular hole system has a difference in speed less than the square hole, but the deviation of the speed of the square hole is still within the limit allow ≤ 20% [3];

- Experiment has proven to allow the diversification of the air distribution grille to be square holes. On the other hand, the square grille system is more cost effective, the same size

and materials, the price of grille system square hole with only about 40% of the round hole grille;

- Experimental results of a two-sided symmetrical grille (V10 and R10) for electrostatic precipitator of CFB boiler with capacity of 55MW have been applied at Cao Ngan Thermo-TKV, have improved precipitator efficiency 1.1% compared with before not applied (before application 98.1%, after application 99.2%).

GENERAL CONCLUSION

1- Electrostatic precipitator physics model has been selected with 2 filter rooms together with modern measuring equipment to measure experimental parameters: air flow, air speed, air pressure and heat the air in the filter chamber;

2- The smallest square has been applied and the mathematical relationship between the air speed error and the distance of the measurement location on a filter section is applied. This allows the assessment of the uniformity of the velocities at different measurement points on the same cross section;

3- The results of calculating the condition coefficient of the experimental regression equations show: $r_{xy} = \hat{a}_1 . \frac{S_x}{S_y}$ and total residual squared $S_{(\hat{a}_0 + \hat{a}_1)} = (n-1) S_y^2 (1 - r_{xy})^2$ qualified. This shows that the uniformity of a very small speed in the filter chamber has reached the deviation between velocities.

In the case of installation of 2 square grille symmetrical matrices (the 2nd option): at the entrance and exit doors, the difference in speed on the same section is quite small (7-17%) and when installing the grille V10 to R10 circular hole system (the 8th option), the speed difference on the same section is very small (3 - 13%) on 4 sections;

5- With the clearance coefficient (45%) of the grille when the grille is equal in number, the circular hole system has a difference in speed less than the square hole, but the deviation of the speed of the square hole is still in the gender allowable limit ≤ 20% [3];

6-Experiment has shown that diversification of the air distribution grille is a square hole instead of the current one in Vietnam using a round hole grille. On the other hand, the square hole grille system is more cost effective, with a square grille system costing only about 40% of the round hole grille due to the square hole system that allows the use of bar material available in water;

7- The experimental results of a two-sided symmetrical grille (V10 and R10) for the static electricity filter of a CFB boiler with the capacity of 55MW have been applied at Cao Ngan Thermo-TKV Thermal Power Company. Dust filtration rate up to 1.1% compared to before (98.1% before application 99.2%).

LIST OF PUBLISHED PROJECTS OF THE THESIS

[1]. Research and propose a set of experimental parameters to improve the efficiency of electrostatic precipitators in coal-fired power plants, Journal of Mechanical Engineering, No. 8, 2014.

[2]. Optimize the flow of air in the filter chamber to improve the efficiency of the electrostatic precipitator, Vietnam Mechanical Journal - No. 7 in 2015.

[3]. Study the effect of air speed level on the efficiency of electrostatic precipitator equipment, Proceedings of the national science and technology conference on mechanics - Fourth.

[4]. Evaluate the influence of some technical parameters of the equatorial grille to the air speed level by Experiment, Journal of Science and Technology, Hanoi University of Industry - No. 40 (June 2017)